Proceedings of the 1992 IEEE
International Conference on Robotics and Automation
Nice, France - May 1992

Human Induced Instability in Powered Hand Controllers

H. Kazerooni and Peter M. Bobgan

Mechanical Engineering Department
University of California, Berkeley, CA 94720, USA

Abstract

This article describes the dynamic behavior of a hand controller when it is maneuvered by a human. A general control architecture is developed which guarantees various impedances on the hand controller. We show that some compliancy either in the hand controller or in the human arm is necessary to achieve stability of the hand controller and the human arm taken as a whole. The actuators' backdrivability, and the dynamics of the hand controller mechanisms are discussed as they relate to system stability. A set of experiments which were performed on a prototype hand controller are presented to show the system performance.

Nomenclature

The Laplace argument, s, for all functions will be omitted throughout this article except when new quantities are defined or when required for clarity.

- $e(s)$ input command to the hand controller
- $f(s)$ force on the hand controller
- $G(s)$ hand controller dynamics
- $H(s)$ human arm dynamics
- $K(s)$ compensator (operating on force, f)
- K_o DC gain of $K(s)$
- τ time constant of $K(s)$
- $x(s)$ hand controller position

1. Introduction

Hand controllers are multi-degree-of-freedom mechanisms which are used to command a variety of machines including, robotic systems, helicopters, and underwater and space vehicles. A hand controller allows multiple commands to be integrated into a single hand movement. The novelty of hand controllers is apparent in maneuvering unmanned underwater vehicles. Traditionally, the speed of the underwater vehicle in various directions is a function of the position of the hand controller in various directions. The operator can control the three dimensional motion of the vehicle from a single handgrip. Hand controllers fall into two categories: passive and active. Passive hand controllers are not powered and do not provide any force feedback to the operator. The passive hand controller consists of linkages, encoders and other passive elements. Some passive hand controller also include springs and dampers in the joints to provide resistance to motion. Reference [13] describes a multi-degree-of-freedom passive hand controller used for helicopter flight control. Reference [6] formulates a helicopter handling quality using a multi-degree-freedom passive hand controller. A fundamental limitation in performance of passive hand controller arises from the operator inability to modulate the hand controller dynamic behavior. This is true because the passive hand controller's behavior is a <u>fixed</u> function of the mechanism dynamics. Active hand controllers, however, include powered actuators in the mechanism joints. The actuator at each joint is used to produce an arbitrary resistance to the operator's motion. This resistance to motion can be modulated to provide different dynamics in different directions. For example, since the human arm is stronger in a pitch motion than a roll motion, pilots usually prefer to feel a large stiffness in the pitch motion and a small stiffness in the roll motion. In another example, the hand controller may have to be rolled and pitched along arbitrary pivots that are not located at the same point. Note that the axes of the coordinate frame for a desired dynamic behavior (impedances), in general, do not coincide with the hand controller's motors' axes; these desired impedances must be developed electronically. See references [4 and 12] for description of two novel powered hand controllers.

Powered hand controllers are of paramount importance in force reflecting systems [14]. In these systems, the hand controllers resistance to motion is a function of the forces applied to the controlled machine. For example, in maneuvering an unmanned underwater vehicle with a force reflecting hand controller, the position of the hand controller would correspond to the velocity of the vehicle and the force on the hand controller would correspond to the drag forces on the vehicle. In another example, a force

0-8186-2720-4/92 $3.00 ©1992 IEEE

reflecting hand controller is the master in a master-slave telerobotic system. "Telepresence" denotes a dynamic behavior in telerobotic systems in which the environmental effects experienced by the slave are transferred through the master to the operator without alteration; therefore, the human feels that he/she is "there" without "being" there. See references [1, 2, 5] for the role of force reflection in telemanipulations.

This article is concerned with the stability of a powered hand controller interacting with a human arm. Section 2 describes the hand controller and the human arm dynamic behavior. Sections 3 and 4 introduce the control architecture and the stability condition. Section 5 describes the trade-offs between the stability and performance via a set of experiments.

2. Modeling

This section models the dynamic behavior of the hand controller and the human arm.

<u>Hand Controller</u>

The hand controller is assumed to have a closed-loop position controller. A closed-loop position control system minimizes the effects of frictional forces in the joints and in the transmission mechanism, and creates a more definite dynamic behavior in the mechanism. Minimizing the effects of uncertainty in electromechanical systems is a usual design specification for position controllers. (See reference [15] for a design method). A closed-loop position control system creates linear dynamic behavior in the hand controller. Here it is assumed that, for non-linear hand controller dynamics, a nonlinear stabilizing controller has been designed to yield a nearly linear closed-loop position system for the hand controller. This lets us assume that the hand controller closed-loop dynamics can be approximated by transfer functions.

The end-point position of the hand controller is a dynamic function of both its input command, e, and the human force, f. The structure of the positioning controller is not of importance in this analysis. G and S are two transfer functions that relate the hand controller end-point position, x, to the input command, e, and the human force, f.

$$x = G\,e + S\,f \qquad (1)$$

The motion of the hand controller end-point in response to imposed forces (f) is caused by either structural compliance in the hand controller or by the compliance of the positioning controller. S is called the sensitivity transfer function, and it maps the external forces to the hand controller position. Whenever an external force is applied to the hand controller, the end-point of the hand controller will move in response. If the hand controller has a "good" positioning controller, the change in position due to the external force will be "small" as long as the magnitude of the external force lies within certain limits. Note that G and S depend on the nature of the closed loop controller. If a compensator with several integrators is chosen to insure small steady state errors, then S will be small in comparison to G. If the hand controller actuators are non-backdrivable, then S will be small regardless of how carefully the hand controller's positioning compensator is chosen.

<u>Human Arm Dynamics</u>

The force imposed by the human arm on the hand controller results from two inputs. The first input, m, is the force imposed by the human muscles[1], the second input is the motion of the hand controller. If the hand controller is stationary, the force imposed on the hand controller is a function only of muscle forces. However, if the hand controller moves, the force imposed on the hand controller is a function not only of the muscle forces but also of the motion of the hand controller. In other words, the human contact force with the hand controller will be disturbed and will be different from m, if the hand controller is in motion. H is defined in equation 2 to map the hand controller position, x, onto the contact force, f.

$$f = m - H\,x \qquad (2)$$

H is the human arm impedance and is determined primarily by the physical properties of the human arm. This model is in agreement with the modeling described in Reference [16]. Figure 1 depicts how the hand controller and human interact dynamically.

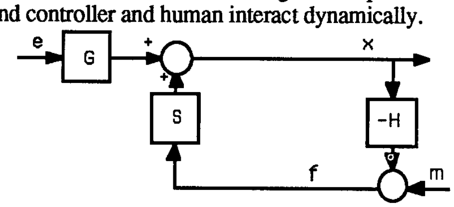

Figure 1: Hand Controller and Human Arm

3. The Control Architecture

Figure 2 shows the system when force compensator, K, is incorporated in the control structure. When the hand controller is not in contact with the human, the actual position of the hand controller end-point is governed by equation 1, where $f = 0$. The feedback loop on the contact force f closes naturally when the hand controller encounters the human arm. Examining figure 2 reveals that K

---

1 It is assumed that the specified form of m is not known other than that it is the result of neural commands deciding to impose a force onto the hand controller. The dynamic behavior in the generation of m by the human central nervous system is of little importance in this analysis since it does not affect the system performance and stability [3, 7].

provides additional paths for f to map to x. The physical contact between the human and the hand controller produces some hand controller motion as f acts through S. In general, S is small: thus, the human operator alone does not have sufficient strength to move the hand controller as desired. An additional route for f to map to x can be added if K is chosen to be non-zero; K can be thought of as the component that shapes the overall mapping of the force f to the position x. This leads to an effective sensitivity of (S + G K).

G and S are fixed by the mechanical design of the hand controller and by the chosen position controller. The designer has some freedom (limited by stability considerations) to adjust the effective sensitivity (S + G K) along the path from f to x; (S + G K) affects how the hand controller "feels" to the human operator. For instance, if K is chosen so (S + G K) is approximately a constant, the hand controller reacts like a spring in response to f. Similarly, if (S + G K) is approximately a single or double integrator, the hand controller acts like a damper or mass, respectively. A large value for K develops a compliant hand controller while a small K generates a stiff hand controller. One cannot choose arbitrarily large values for K; the stability of the closed-loop system of Figure 2 must also be guaranteed.

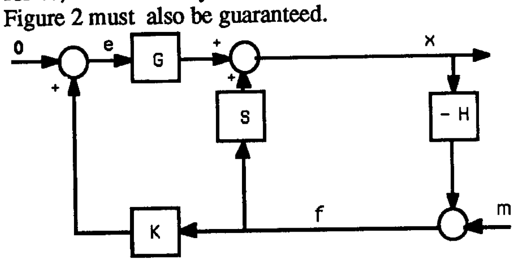

Figure 2: Addition of a Force Compensator

4. The Closed-Loop Stability

The Nyquist Theorem is used to develop a sufficient stability condition for the closed-loop system in Figure 2. This sufficient condition results in a class of compensator K which guarantees the stability of the closed-loop system. Note that the stability condition derived in this section does not give any indication of system performance, but only ensures a stable system.

According to the Nyquist criterion, the system shown in Figure 2 remains stable as long as

$$|GKH| < |1+SH| \quad \forall \omega \in [0, \infty) \quad (3)$$

Or: $|GK| < |S + 1/H| \quad \forall \omega \in [0,\infty) \quad (4)$

Inspection of inequalities 3 and 4 show that the smaller the sensitivity of the hand controller, the smaller K must be. Also from inequality 4, the more rigid the human arm is, the smaller K must be. In the "limiting case" when the hand controller is infinitely stiff [S = 0], no K can be found to enable interaction with an infinitely rigid human arm [$H \rightarrow \infty$]. In other words, for stability of the system shown in Figure 2, there must be some compliancy either in the hand controller or in the human arm. The hand controller compliancy may be due to structural flexibility, and/or the electronic compliancy resulting from the positioning controller. The stability condition for multi-degree-of-freedom (when G, K, H, and S are transfer function matrices) can be derived in a similar way using singular values.

$$\sigma_{max}[G K H] < \sigma_{min}[I + S H] \quad \forall \omega \in [0,\infty) \quad (5)$$

Transmission systems with large transmission ratios are not backdrivable and result in small sensitivity functions (S). We suggest that the hand controllers be designed to be backdrivable. This can be done by employing low-ratio transmission systems to drive the hand controller. Direct drive systems, because of the elimination of the transmission systems, can potentially have large S.

Another method of increasing S is to decrease the position controller gain. The decrease in the position control gain may result in a sluggish response for the hand controller. However, we suggest that this gain be chosen to be as small as possible. In particular, we recommend that integral control must be avoided in the position control loop. Our previous experiments [9, 10] have shown that a 5-hertz bandwidth for K is sufficient for most maneuvers. The suggested form of K is given by equation 6.

$$K = \frac{K_o}{\tau s + 1} \quad (6)$$

5. Experiment

Figure 3 shows the experimental one-degree-of-freedom electrically powered hand controller. Using the encoders for feedback, a primary stabilizing controller for the hand controller is designed to yield the widest bandwidth for the closed-loop position transfer function, G, and yet guarantee the stability of the closed-loop positioning system in the presence of bounded unmodeled dynamics in the hand controller and harmonic drive. The development of the position controllers for the hand controller has been omitted for brevity. An experimental plot of G with the bandwidth of 10 rad/sec is given in Figure 4. A human arm model was derived to verify the stability condition. The model derived for the human arm does not represent the human arm sensitivity H for all configurations of the arm; it is only an approximate and experimentally verified model of the author's arm in the neighborhood of the Figure 3 configuration. For the experiment, the author gripped the handle, and the hand controller was commanded to oscillate via sinusoidal functions. At each oscillation frequency, the operator tried to move his hand to follow the hand controller so that zero contact force was maintained between his hand and the hand controller. Since the human arm cannot keep up with the high-frequency motion of the hand controller when trying to maintain zero contact forces, large contact forces and consequently, a large H are expected at high frequencies. Since this force is equal to the product of the hand controller acceleration and human arm inertia (Newton's Second Law), at least a second-order transfer function is expected for H at high frequencies. On the other hand, at low frequencies (in particular at DC), since the operator can follow the hand controller motion comfortably, he can always establish almost constant contact forces between his hand and the hand controller. This leads to the assumption of a constant transfer function for H at low frequencies where contact forces are small for all values of hand controller position. Based on several experiments, the best estimates for the author's hand sensitivity is presented by equation 7.

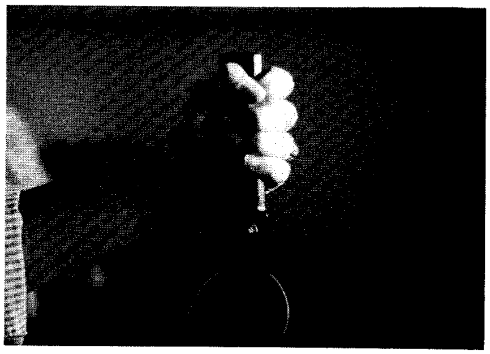

Figure 3: One-Degree-of-Freedom Hand Controller

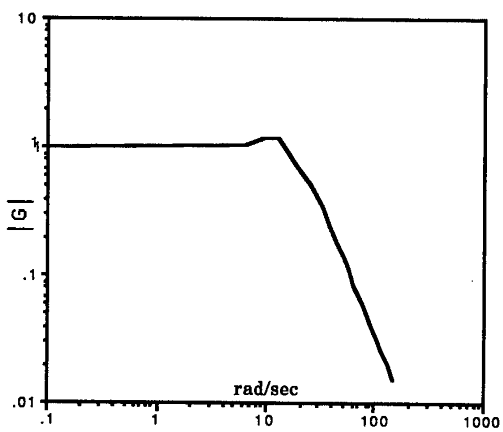

Figure 4: Hand Controller Dynamics

$$H = \left[\frac{s^2}{20} + \frac{s}{5} + \frac{1}{5}\right] \quad \text{lbf-ft/rad} \qquad (7)$$

Figure 5 shows the experimental values and the fitted transfer functions (equation 7) for the human arm dynamic behavior.

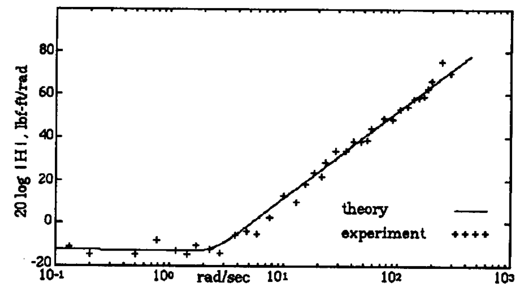

Figure 5: Human Arm Dynamic s in the in the Neighborhood of the Figure 4 Configuration

<u>Performance with low frequency maneuvers</u>

A set of experiments were performed to show how the hand controller sensitivity can be shaped. In particular the objective was to make the hand controller behave like a spring: the hand controller deviation from its equilibrium position is proportional to the imposed force. Inspection of Figure 2 reveals that: $x = (S + GK)f$ where $(S + GK)$ represents the total sensitivity of the hand controller. K must be chosen such that $(S + GK)$ becomes equal to the desired sensitivity while the system stability is guaranteed. Since G (shown in Figure 4) is constant within its bandwidth, we choose K as a first order transfer function (equation 6) with a bandwidth larger than the bandwidth of G. This results in a constant overall sensitivity, $(S + GK)$, within the bandwidth of G. Figure 6 shows f vs x for various values of K_o when the operator pushes the hand controller uniformly. In all cases the value of K_o (the maximum value of K for all frequencies) was less than $1/H$ satisfying the stability condition in inequality 4. The slope of each plot in Figure 6 represents the hand controller overall sensitivity or $(S + GK)$. Since S is small and G is unity within its bandwidth, the slope of each plot represents K_o.

<u>Performance with high frequency maneuvers</u>

In another set of experiments, the operator maneuvers the hand controller irregularly (i.e., randomly). Figure 7 shows the history of the hand controller position, x, and the human force, f, as functions of time where $K_o = 0.1$ satisfying the stability condition in inequality 4. Irregular maneuvers create high and low frequency components in the hand controller motion. Figure 8 shows the measured force, f, versus x where the slope of 0.1 implies that the desired sensitivity of $K_o = 0.1$ has been achieved within the system bandwidth.

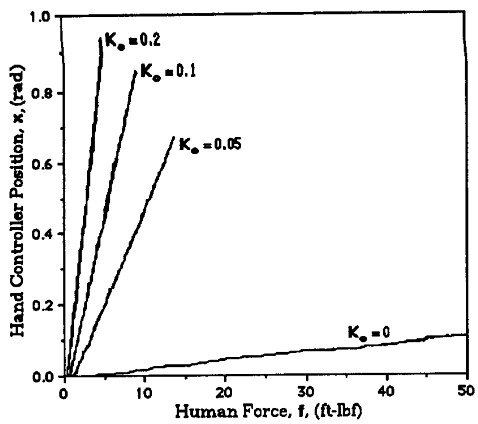

Figure 6: By Choosing K, the hand controller sensitivity function, [S + GK] can be shaped.

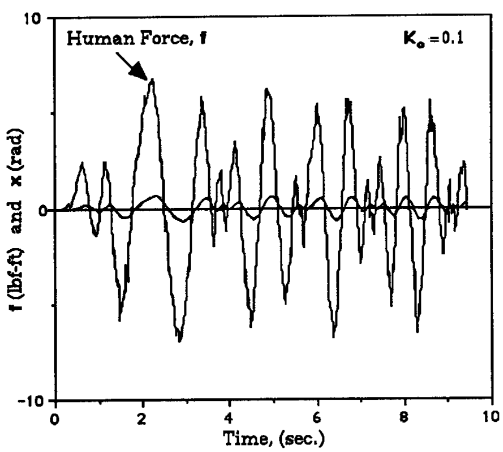

Figure 7: x = 0.1 f within the bandwidth

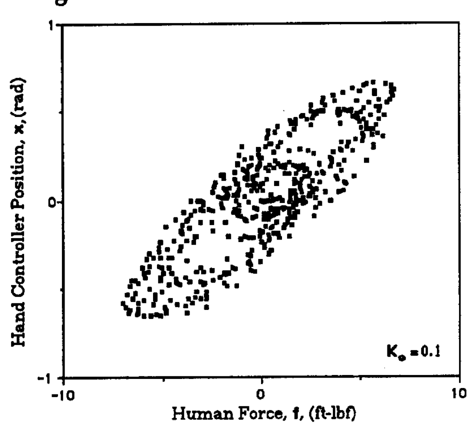

Figure 8: The average slope of 0.1 reveals that x =.1 f for frequencies within the bandwidth.

<u>Stability Condition</u>

A set of experiments were carried out to verify the stability condition. K was chosen to be:

$$K = \frac{Ko}{[s/2 + 1]^2}$$

Figure 9 shows GK for various values of K_o; it can be observed that for all values of K_o smaller than 5, $|GK| < |1/H|$, and satisfies the stability condition (inequality 4). Figure 10 shows the system response (x and f) when $K_o = 3$ satisfying the stability condition. Figure 11 shows the measured force, f, versus x where the slope of 3 implies that the desired sensitivity of $K_o = 3$ has been achieved within the system bandwidth. Figure 12, however, shows a maneuver where $K_o = 5$ violated the stability criterion; resulting in the unstable system.

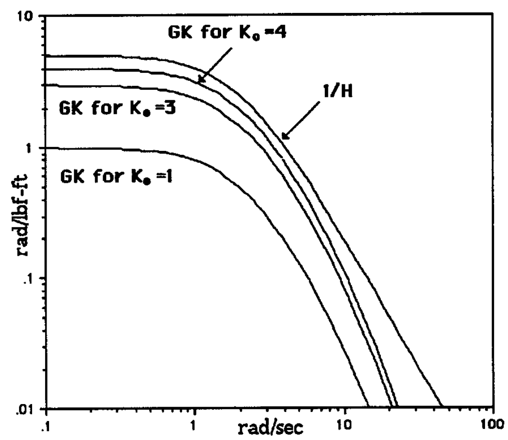

Figure 9: For all values of K_o smaller than 5, $|GK|$ is smaller than $|1/H|$ satisfying 4.

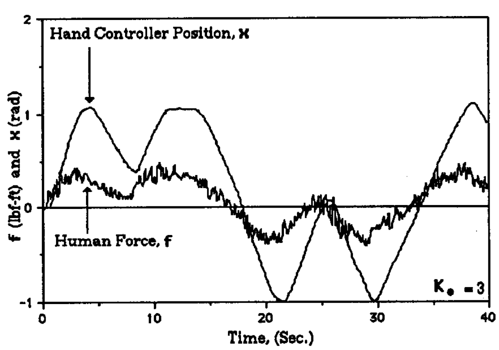

Figure 10: The stable time history of the human force, f, and the hand controller position, x.

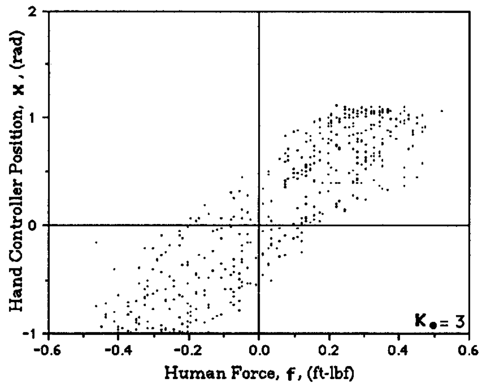

Figure 11: The average slope of 3 reveals that x = 3 f for all frequencies within the bandwidth.

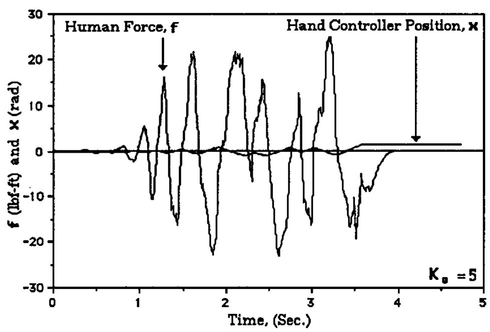

Figure 12: The unstable time history of the human force, f, and the hand controller position, x, when the controller violates the stability condition.

6. Conclusion

A control architecture has been given to develop compliancy in a hand controller. It has been shown that for the stability of the hand controller and the human arm taken as a whole, there must be some compliancy either in the hand controller or in the human arm. A single-degree-of-freedom powered hand controller has been built for theoretical and experimental verification of the hand controller dynamics. A set of experiments are given to verify the system performance and stability condition.

7. References

1) Bejczy, A. K., Handlykken, M., "Experimental Results with a Six Degree-of-Freedom Force Reflecting Hand Controller, *17th Annual Con. on Manual Control*, Los Angeles, CA, June 81.
2) Bejczy, A. K., Bekey, G., Lee, S. K., "Computer Control of Space Borne Teleoperators with Sensory Feedback", *IEEE Con. on Robotics and Auto.*, 85.
3) Berthoz, A., Metral, S., "Behavior of Muscular Group Subjected to a Sinusoidal and Trapezoidal Variation of Force", J. of App. Physiol., V29, 70.
4) Bruno, J. M., "The JAU-JPL Anthropomorphic Telerobot", in Proceedings of the NASA Conference on Space Telerobotics, V. IV, Jan. 89.
5) Chapel, J. D., "Performance Limitations of Bilateral Force Reflection Imposed by Operator Dynamic Characteristics", NASA Conference on Space Telerobotics, V. IV, Jan 1989.
6) Glusman, S. I., Landis, K. H., Dabundo, C., "Handling Qualities Evaluation of the ADOCS Primary Flight Control System", 42nd Annual Forum of the American Helicopter Society, Washington, DC, June 1986.
7) Houk, J. C., "Neural control of muscle length and tension", in: Motor control, ed. V. B. Brooks. Bethesda, MD, American Physiological Society Handbook of Physiology.
8) Jacobsen, S. C., Iversen, E. K., Knutti, D. F., Johnson, R. T., Biggers, K., "Design of the Utah/MIT Dextrous Hand", IEEE International Conf. on Robotics and Automation, April 1986.
9) Kazerooni,H., "Human-Robot Interaction via the Transfer of Power and Information Signals," IEEE Transactions on Systems and Cybernetics, Vol. 20, No. 2, March 1990.
10) Kazerooni, H., Mahoney, S. M., "Dynamics and Control of Robotic Systems Worn by Humans", IEEE International Conference on Robotics and Automation, Sacramento, CA, May 1991.
11) Lehtomaki, N.A., Sandell, N.R., Athans, M., "Robustness Results in Linear-Quadratic Gaussian Based Multivariable Control Designs", IEEE Trans. on Auto. Control, Vol. AC-26, No. 1, Feb. 1981.
12) Lindemann R., Tesar, D., "Construction and Demonstration of a 6 DOF Force Reflecting Joystick for Telerobotics", NASA Conf. on Space Telerobotics, Vo.IV, Jan. 89.
13) Lippay, A. L., King M., Kruk R. V., Morgan, M., "Helicopter Flight Control with One Hand", Canadian Aeronautiocs and Space Journal, Vo. 31, No. 4, December 1985.
14) Repperger, D. W., "Active Force Reflection Devices in Teleoperation", IEEE Control Systems, Vol. 11, No. 1, January 91.
15) Spong, M.W. and Vidyasagar, M., "Robust Nonlinear Control of Robot Manipulators," *Proc. 24th IEEE Conf. on Decision and Control*, Ft. Lauderdate, Florida, 1767-1772, December 1985.
16) Stein, R. B., "What muscles variables does the nervous system control in limb movements?", J. of the behavioral and brain sciences, 1982, V.5.

This research work was supported by a grant from NSF under contract IRI-9103955.